
AV-data2vec: Self-supervised Learning of Audio-Visual Speech Representations with Contextualized Target Representations

Jiachen Lian¹ Alexei Baevski^{*2} Wei-Ning Hsu^{*2} Michael Auli^{*2}

Abstract

Self-supervision has shown great potential for audio-visual speech recognition by vastly reducing the amount of labeled data required to build good systems. However, existing methods are either not entirely end-to-end or do not train joint representations of both modalities. In this paper, we introduce AV-data2vec which addresses these challenges and builds audio-visual representations based on predicting contextualized representations which has been successful in the unimodal case. The model uses a shared transformer encoder for both audio and video and can combine both modalities to improve speech recognition. Results on LRS3 show that AV-data2vec consistently outperforms existing methods under most settings.

1. Introduction

Both human speech production and perception are multi-modal, producing acoustic and visual artifacts (Diehl et al., 2004; Hockett & Hockett, 1960). The human brain also processes speech as a combination of auditory, visual, and even tactile stimuli (McGurk & MacDonald, 1976; Calvert et al., 1997; Musacchia et al., 2006; Fowler & Dekle, 1991). This is in stark contrast to state-of-the-art speech recognition research which focuses mostly on the audio signal to perform tasks such as automatic speech recognition (ASR; Gulati et al. 2020; Baevski et al. 2020; Hsu et al. 2021; Chen et al. 2022a; Baevski et al. 2022b; Radford et al. 2022).

There is a growing body of work on learning *audio-visual speech representations*. The idea is to process speech audio together with visual cues such as lip movement, facial expressions, body language, and other nonverbal behaviors (Summerfield, 1992; Bernstein & Liebenthal, 2014). The visual information helps to improve the robustness and

accuracy of speech recognition in both noisy and clean settings (Shi et al., 2022a;b). This joint processing is typically referred to as audio-visual speech recognition (AVSR). However, processing only the visual signal in visual speech recognition (VSR) also has important applications such as supporting people which lost their ability to speak due to various reasons (Seddik et al., 2013).

The state-of-the-art VSR system relies on about 90K hours of transcribed training data (Serdyuk et al., 2022). However, annotating such large amounts of data for every language is simply infeasible which sparked large interest to learn from unlabeled data. AV-HuBERT (Shi et al., 2022a) was the first self-supervised system to jointly learn speech representations from raw audio and video using masked-prediction. However, the training is not entirely end-to-end since the algorithm alternates between representation learning and creating targets using offline clustering. More recently, Haliassos et al. (2022) introduced an end-to-end algorithm similar to data2vec (Baevski et al., 2022b) which trains separate encoder models for audio and visual data. However, separate encoders increase the number of model parameters and their disjoint model design is also contradictory to the common understanding of the human perception system which is believed to fuse audio and vision early on (Green, 1998). Moreover, they do not explore AVSR which tends to perform better than ASR (Shi et al., 2022b; Hsu & Shi, 2022).

In this paper, we introduce AV-data2vec (Audio-Visual data2vec) to address these issues by extending data2vec (Baevski et al., 2022b) from the unimodal case to learn joint audio-visual representations (Figure 1). AV-data2vec encodes masked audio-visual data and performs a masked prediction task of contextualized targets based on the unmasked input data. Compared to prior work, training is fully end-to-end and there is a single encoder for both audio and vision that can be used to perform AVSR. Another difference to RAVen (Haliassos et al., 2022) is that target representations include features of varying granularity which is achieved by averaging the outputs of multiple layers instead of only predicting high-level features produced by the final layer. This enables a learning task over both low-level and high-level features. Results on LRS3 show that AV-data2vec consistently outperforms existing

^{*}Equal advising ¹University of California, Berkeley. Work done at Meta AI. ²Meta AI. Correspondence to: Jiachen Lian <jiachenlian@berkeley.edu>.

self-supervised audio-visual learning frameworks in most settings.

2. Related Work

Self-supervised Speech Representation Learning.

There has been much recent research on self-supervised speech representation learning which includes approaches that reconstruct a corrupted or incomplete form of the input using auto-encoding (Van Den Oord et al., 2017), auto-regressive based methods such as Chung & Glass (2020); Chung et al. (2020); Ling et al. (2020), and masked prediction based methods (Yue & Li, 2021; Liu et al., 2020). Another line of work maximizes the similarities of positive pairs of embeddings and minimizes the similarities of negative pairs of embeddings in the latent space (Oord et al., 2018; Schneider et al., 2019; Baevski et al., 2019b; 2020). There is also work on predicting the frame-wise targets outside of the model computational graph (Baevski et al., 2019a; Hsu et al., 2021; Chen et al., 2022a). Related to the current paper is Baevski et al. (2022b;a) who directly regress contextualized and continuous targets created by a teacher model. Contextualization can capture the information of the entire sequence in the latent target representation.

Self-supervised Multi-modal Training. A lot of recent attention has been devoted to self-supervised learning over multiple modalities such as vision (image and video), text, and speech. Multi-modal training enables to ground each modality in another modality through a cross-modal learning task. This line of work includes image-text pretraining (Li et al., 2019; Wang et al., 2021; Radford et al., 2021; Alayrac et al., 2022; Dou et al., 2022; Zeng et al., 2021; Yang et al., 2022; Li et al., 2022). Many explorations have also been made in video-text pretraining such as Sun et al. (2019); Luo et al. (2020); Xu et al. (2021); Luo et al. (2021); Fang et al. (2021). There are also numerous investigations taking place in the realm of speech tasks such as Bapna et al. (2021); Ao et al. (2021); Zhang et al. (2022); Chen et al. (2022b) in speech-text pretraining, Chan et al. (2022); Shi et al. (2022a;b); Hsu & Shi (2022); Haliassos et al. (2022) in speech-video pretraining, and Akbari et al. (2021); Zellers et al. (2022) speech-text-video pretraing.

Speech Recognition With Visual Cues. Visual-oriented speech recognition involves the task of *visual speech recognition* (VSR, also known as lip reading) and *audio-visual speech recognition* (AVSR). Earlier work (Afouras et al., 2018a; Xu et al., 2020; Shillingford et al., 2018; Ma et al., 2022; Makino et al., 2019; Prajwal et al., 2022; Serdyuk et al., 2021; 2022) in visual-oriented speech recognition started to train with transcribed video/audio-video data in a supervised manner. However, this required large amounts of

labeled data of up to 90K hours (Serdyuk et al., 2022). There are some semi-supervised methods (Afouras et al., 2020; Ma et al., 2022) which significantly reduce the amount of labeled data, however, the performance is still far lower.

Most recent advances in self-supervised audio-visual learning (Shi et al., 2022a;b; Hsu & Shi, 2022; Haliassos et al., 2022) are not only more data-efficient but also achieve comparable or better speech recognition results. AV-HuBERT (Shi et al., 2022a) is the first method that jointly learns the modality-agnostic speech representation from raw audio and video. u-HuBERT (Hsu & Shi, 2022) generalizes AV-HuBERT to utilize both multimodal and unimodal data that is richer in the wild during pretraining. Additionally, it unifies fine-tuning with a modality-agnostic objective, achieving comparable or better results than modality-specific objectives. VATLM (Zhu et al., 2022) extends AV-HuBERT by adding auxiliary speech-text tasks which use large amount of additional out-of-domain text and speech data in an either multimodal or unimodal manner.

One problem with these approaches is that multi-stage iterative training with offline clustered labels is not end-to-end. RAVen (Haliassos et al., 2022) uses a student-teacher paradigm (Grill et al., 2020; Caron et al., 2021) and is end-to-end, however, it uses separate encoders for each modality. This is less parameter-efficient and very different to the human speech perception mechanism which is believed to fuse modalities early on (Green, 1998). Furthermore, AVSR (Shi et al., 2022b; Hsu & Shi, 2022), which tends to outform ASR consistently, is not deployable in RAVen.

3. Method

3.1. Background: data2vec

data2vec (Baevski et al., 2022b;a) is a self-supervised framework that learns the representations from *contextualized* targets via masked prediction. Specifically, a student model encodes a masked version of the training example to predict a contextualized target representation encoded by a teacher model which is based on the unmasked version of the sample. The teacher model weights are an exponentially moving average (EMA) of the student model weights (Grill et al., 2020; Caron et al., 2021). data2vec is a general learning criterion that can be applied to multiple modalities such as vision, language and speech. The original data2vec framework is designed for single-modality training and we refer to it as *unimodal* data2vec.

3.2. Audio-Visual data2vec

We extend unimodal data2vec to multiple modalities and focus on speech and video inputs to create joint audio-visual representations (Fig. 1). Similar to data2vec, AV-data2vec has a *student encoder* and a *teacher encoder*, however, in-

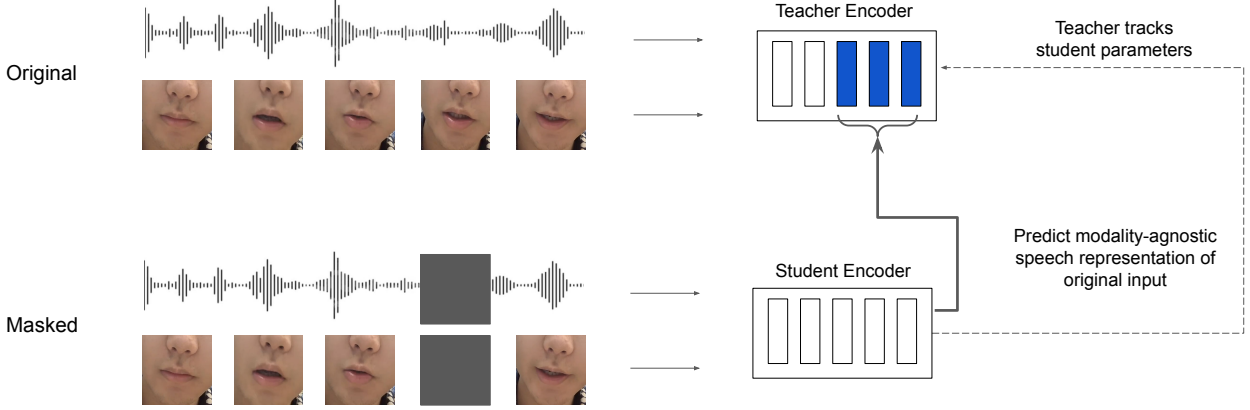


Figure 1. AV-data2vec jointly encodes both audio and visual data to build audio-visual representations. The student model encodes a masked version of both the audio and visual data and predicts a contextualized target representation created by a teacher model which is based on the unmasked version of the training sample. Target representations encode both high-level and low-level features from multiple layers of the teacher model. In this example, the target representation is the average of the outputs of the last three layers.

stead of processing a single modality, encoders can represent both audio and visual data. The input to the student encoder is a masked version of both the audio and video data based on which the student network tries to predict contextualized target representations. These targets are created by a teacher encoder to which the unmasked version of the the same data is fed. Both the student and teacher networks are composed of an audio encoder A , a video encoder V , a audio-visual fusion module F and a transformer encoder T .

Audio Encoder. Similar to Shi et al. (2022a), we encode the audio signal as log filterbanks. We then adopt a dense layer as audio encoder A that maps the U -frame log filterbank energy $X_A = [x_1, x_2, \dots, x_U]$ to acoustic features $M_A = [M_1, M_2, \dots, M_U] \in \mathbb{R}^{U \times D}$ of the same length: $M_A = A(X_A)$. The feature dimension D of the audio encoder matches the input dimension of the transformer encoder. The audio feature M_A is normalized per frame statistics for both pretraining and finetuning (Shi et al., 2022a).

Video Encoder. We use the same video encoder V as AV-HuBERT which is a variant of ResNet-18 (Ma et al., 2022; Shi et al., 2022a; Haliassos et al., 2022; Zhu et al., 2022) that replaces the first 2D convolutional layer (He et al., 2016) by a 3D convolutional layer with a kernel size $[5, 7, 7]$ (Petridis et al., 2018), followed by a batch-norm 3D layer (Ioffe & Szegedy, 2015), a PRelu layer (He et al., 2015) and a MaxPooling 3D layer with kernel size $[1, 3, 3]$ and strides $[1, 2, 2]$. The visual features are then reshaped in order to be input to the subsequent 16-layer 2D convolutional layers (He et al., 2016). An adaptive average pooling 2D layer is applied in the end to output a 1D tensor for each frame. Given a U -frame raw

video signal $X_V = [x_1, x_2, \dots, x_U] \in \mathbb{R}^{U \times C \times H \times W}$, the visual encoder V maps X_V to 1D visual features $M_V = [M_1, M_2, \dots, M_U] \in \mathbb{R}^{U \times D}$: $M_V = V(X_V)$ Both the dimension D and number of frames T of visual encoder are the same as those of audio encoder. C , W , and H denote channel, weight and height of each video frame.

Audio-Visual Fusion. AV-data2vec accepts inputs that are either audio-only (a), video-only (v), or audio-video (av) for both student and teacher models. This leads to nine possible training tasks.¹ This compares to four learning tasks for RAVen (Haliassos et al., 2022) whose encoders can only encode a single modality each and which lacks the ability to jointly encode modalities. AV-HuBERT (Shi et al., 2022a) can jointly encode modalities and uses *modality dropout* to randomly select the type of input. In initial experiments, we found it very beneficial to adjust the rate at which each input type is selected over time during training.

In this work, we propose a new modality scheduler that coordinates the nine different training tasks. We define the following parameters: p_A , p_V and p_{AV} , denoting the probability that audio/video/audio-video is selected as input modality respectively for either the student or the teacher.²

Early results (Sec.5.5) showed that audio-only targets performed best in our setup. We designed a modality dropout scheduler *for the student model* where the rate at which modalities are dropout change over the time. The probabil-

¹v→a, av→v, a→a, v→v, av→v, a→v, v→av, av→av, a→av, where → denotes student-to-teacher prediction.

²In the actual implementation, either audio or video is selected conditioned on audio-video not being selected. More precisely: $p_A = p_{AV} p_{A|AV}$ and $p_V = p_{AV} p_{V|AV}$, where $p_{AV} = 1 - p_{AV}$

ities p_{AV} , $p_{V|\bar{AV}}$ and $p_{A|\bar{AV}}$ are annealed: given a starting and an ending value for a probability, we linearly anneal the probability over M_{anneal} steps. This results in p_A and p_V to be quadratically annealed over M_{anneal} steps.

The audio-visual fusion module is summarized in Eq. 1. Note that there are two independent audio-visual fusion modules for both the student model and the teacher model.

$$M = \begin{cases} M_A + M_V & \text{with probability } p_{AV} \\ M_A + \mathbf{0} & \text{with probability } p_A \\ M_V + \mathbf{0} & \text{with probability } p_V \end{cases} \quad (1)$$

If the input for both student and teacher model is audio-only data, then this is the same as data2vec (Baevski et al., 2022b) framework for audio (A-data2vec; Sec.5.4).

Masking. Following (Baevski et al., 2020; Hsu et al., 2021), we apply span masking on fused audio-visual features $M = [M_1, M_2, \dots, M_U] \in \mathbb{R}^{U \times D}$. We randomly select $r\%$ timesteps as starting indices to mask spans of length l . Note that if $M = M_A + M_V$, the masking is synchronously applied at the same time step for both audio and video, as illustrated in Fig.1.

Transformer Encoder. The transformer encoder T takes the masked fused audio-visual features \tilde{M} as input (cf. Eq. 1) and outputs the high-level speech representation $Z = T(\tilde{M}) = [z_1, z_2, \dots, z_U] \in \mathbb{R}^{U \times D}$.

3.3. Pretraining Objective

Targets. Similar to Baevski et al. (2022b), AV-data2vec predicts contextualized targets encoding a time-step as well as information about the entire input. Targets are extracted from the representations encoded by the teacher encoder that takes the unmasked features as input. Following Baevski et al. (2022b), we use the output of the FFN prior to the last residual connection in each block as target representation which is denoted as $\bar{Z} \in \mathbb{R}^{U \times D}$. We furthermore denote the target representation at the last k layer as $\bar{Z}^{(N-k+1)} \in \mathbb{R}^{U \times D}$, where N is the total number of transformer blocks, and k is the current block. We then average these representations over the last K blocks and apply instance normalization similar to Baevski et al. (2022b) to derive the targets $Y = \text{IN}(\sum_{k=1}^K \bar{Z}^{(N-k+1)})$, where IN denotes instance normalization.

Loss. Given the outputs of the Transformer encoder $Z = [z_1, z_2, \dots, z_U] \in \mathbb{R}^{U \times D}$ and corresponding contextualized targets $Y = [y_1, y_2, \dots, y_U] \in \mathbb{R}^{U \times D}$ we can compute our objective. We consider computing our loss for both masked time-steps and unmasked time-steps (Haliassos et al., 2022), depending on the input modality. Empirically we find that audio-only targets perform best (§5.5) and in this setting

we found it useful to predict audio targets when we have visual-only inputs even for unmasked time-steps. Whenever we have audio as input, then we only predict targets for unmasked time-steps as the task is otherwise trivial. Specifically, if t is the frame index, I the set of masked indices, α and β are two weighting factors, then the loss is:

$$L_{pretrain} = \alpha \sum_{t \in I} \|z_t - y_t\|_2^2 + \beta \sum_{t \notin I} \|z_t - y_t\|_2^2 \quad (2)$$

Teacher Parameterization Given student encoder weights θ_S , the teacher weights θ_T are an exponentially moving average (EMA) similar to Baevski et al. (2022b):

$$\theta_T \leftarrow \tau \theta_T + (1 - \tau) \theta_S$$

where τ is a momentum parameter that is linearly increased over time $\tau^s \xrightarrow{\tau_{anneal}} \tau^e$, where τ^s , τ^e and τ_{anneal} denote the initial value, the ending value of EMA decay, and the EMA decay annealing steps.

3.4. Finetuning Objective

After pretraining, we initialize the encoder of an attention-based sequence-to-sequence (S2S) architecture (Bahdanau et al., 2016) and finetune it on labeled data. We denote the text targets as $W = [W_1, W_2, \dots, W_S]$ for the current input representation $Z = [Z_1, Z_2, \dots, Z_T]$. We minimize a cross-entropy (CE) criterion: $L_{S2S} = -\sum_{t=1}^S \log(W_t | W_{<t}, Z)$

4. Experimental Setup

4.1. Datasets and Preprocessing

LRS3 (Afouras et al., 2018b) is the largest publicly available labeled dataset for audio-visual speech recognition in English. It was collected from TED and TEDx videos on YouTube and is split as follows: *pretrain* (403h), *trainval* (30h) and *test* (1h). We follow Shi et al. (2022a) to randomly select about 1h of data from *trainval* for validation.

Voxceleb2 (Chung et al., 2018) is a multilingual audio-visual dataset for speaker recognition without transcriptions. The original corpus contains more than 2442 hours of videos. We use the English-only part selected by Shi et al. (2022a) (1326 hours of videos).

Preprocessing. For audio feature extraction, we follow Shi et al. (2022a) and extract the 26-dimensional log filterbank energy with a stride of 10 ms from raw audio waveform. The original video track has a resolution of 224×224 with a frame rate of 25 fps. Following Shi et al. (2022a), we use dlib (King, 2009) to extract 68 facial key points for each video clip. We then crop a 96×96 region centered on the speakers mouth. During training, we randomly crop a 88×88 region from the whole region and flip

it horizontally with probability 0.5. Following Shi et al. (2022a), we only take grayscale images. During testing, we use the 88×88 region centered on the mouth and no flipping is applied. The frame rate of either audio or visual features is unified to be 25 fps. As the original audio features have a frame rate of 100 fps, we stack them for 4 audio features.

4.2. Setup and Implementation Details

We consider two experimental setups in terms of amount of labeled data: *low-resource* and *high-resource*. We pre-train AV-data2vec with either LRS3 (433h) or English-only Voxceleb2 + LRS3 (1759h). In the low-resource setting, the model is finetuned on LRS3 *trainval* (30h) only and in the high-resource setting, the model is finetuned on the entire LRS3 training data (433h). Our methods are implemented in fairseq (Ott et al., 2019).

Pretraining. Following Devlin et al. (2018); Shi et al. (2022a); Zhu et al. (2022), there are two options for transformer encoder: Base and Large. The number of blocks/embedding dimension/feed-forward dimension/attention heads in each transformer block are 12/768/3072/12 and 24/1024/4096/16 for Base and Large respectively. For masking, we set mask probability $r\% = 50\%$ and span length $l = 10$. For pretraining loss defined in Eq.2, we set $\alpha = 1$ and $\beta = 0$ if the input modality is audio-only or audio-video, and if the input modality is video-only, we set $\alpha = 1$ and $\beta = 1$. For student modality scheduler, we set $p_{AV} : 1 \xrightarrow{150k} 0.25$, $p_{V|AV} : 1 \xrightarrow{150k} 1$, $p_{A|AV} : 0 \xrightarrow{150k} 0$. The visualization of the scheduler is given in Appendix. 8.

For teacher modality scheduler, we set the input as audio-only. We fixed these modality schedulers for all pretraining experiments. For BASE model with 433h pretraining, we set $lr=5e-4$, $\tau^s = 0.999$, $\tau^e = 0.99999$, $\tau_{anneal} = 100k$. The batch size is 20s per GPU. We set total number of updates as 1000k and the model is trained on 64 V100 for 4-5 days. For Base model with 1759h pretraining, we use almost the same settings with the exception that we double the effective batch size and train it for 2000k updates (8-10 days). For Large model with 433h pretraining, we still use the same settings as Base model with the exception that we double the effective batch size and $lr=2e-4$. It takes around 6-7 days to finish. For Large model with 1759h pretraining, we use the same settings as Base model with 1759h pretraining with the exception that we set $lr=2e-4$. It takes around 10-12 days to finish training. Details about pretraining hyper-parameters search are discussed in Sec.5.5.

Finetuning. Following Shi et al. (2022a), we consider two configurations of transformer decoders: Base and Large. The number of blocks/embedding dimension/feed-forward

dimension/attention heads in each transformer block are 6/768/3072/4 and 9/1024/4096/8 for Base and Large respectively. We use subword (Kudo, 2018) for S2S targets. For ASR/VSR finetuning, the video or audio features are set as zero vectors respectively. For AVSR finetuning, both video and audio are taken as input and there is no modality dropout. For ASR finetuning, we use tri-stage learning rate scheduler and freeze the encoder for some steps (Shi et al., 2022a). The learning rate/total number of updates/warmup steps for 30h/433h are $1e-3/1e-3$, 40k/60k, 10k/20k, 24k/48k respectively. Settings are the same for both Base and Large model.

For VSR finetuning, we use cosine learning rate scheduler and freeze the encoder for some steps (Shi et al., 2022a). The learning rate/total number of updates/warmup steps for 30h/433h are $1e-3/1e-3$, 40k/120k, 2k/20k, 24k/48k respectively. Settings are the same for both Base and Large model. For AVSR finetuning, we use tri-stage learning rate scheduler and freeze the encoder for some steps (Shi et al., 2022a). The learning rate/total number of updates/warmup steps for 30h/433h are $1e-3/1e-3$, 40k/60k, 10k/20k, 24k/48k respectively. Settings are the same for both Base and Large model. Since the AVSR results are not reported in Shi et al. (2022a) and are partially reported in Shi et al. (2022b), we reproduced AV-HuBERT and report our own AVSR results for the remaining settings, shown in Table.1 and Table.2.

Decoding. We simply tune the beam width among $\{5, 10, 25, 50, 100\}$ and report the best number. We do not apply LM for decoding. For VSR, ASR and AVSR tasks, the input modalities are video-only, audio-only and audio-video respectively in both finetuning and decoding.

5. Results

5.1. Low-labeled Data Setup

We first consider a low-labeled data setup using 30h of data for finetuning whose results are shown in Table. 1. For Base models, AV-data2vec consistently outperforms existing methods for both VSR and ASR. On AVSR, AV-data2vec achieves the best result except for the 433h pretraining setting, where AV-data2vec achieves 4.2 compared to 3.6 for VATLM. However, VATLM (Zhu et al., 2022) uses additional audio and text data for their auxiliary pretraining tasks. AV-data2vec appears to benefit more from an increased amount of pretraining data (1759h vs. 433h) than other approaches.

For Large models, AV-data2vec achieves the best results except for the 1759h setting, where AV-data2vec gets 2.7 while RAVen gets 2.6. We attribute this in part due to RAVen having about double the model size due to their two encoder architecture. Overall, with the same amount of pretraining

Table 1. Low-labeled Data Results. We pretrain AV-data2vec Large/Base with 433h/1759h of unlabeled data, and finetune on 30h of labeled data. The results of visual speech recognition (VSR), automatic speech recognition (ASR) and audio-visual speech recognition (AVSR) are shown. CE denotes cross-entropy, also applying to Table. 2. AV-data2vec achieves state-of-the-art results in most settings.

Methods	Unlabeled AV data	Labeled Data	Encoder Size	Criterion	VSR	ASR	AVSR
<i>Self-supervised (Base Models)</i>							
AV-HuBERT (Shi et al., 2022a)	433h	30h	103M	CE	51.8	4.9	4.7 ²
RAVen (Haliassos et al., 2022)	433h	30h	97M	CTC+CE	47.0	4.7	-
VATLM (Zhu et al., 2022)	433h ¹	30h	103M	CE	48.0	-	3.6
AV-data2vec	433h	30h	103M	CE	45.2	4.4	4.2
AV-HuBERT (Shi et al., 2022a;b)	1759h	30h	103M	CE	46.1	4.6	4.0
RAVen (Haliassos et al., 2022)	1759h	30h	97M	CTC+CE	40.2	3.8	-
VATLM (Zhu et al., 2022)	1759h ¹	30h	103M	CE	42.6	-	3.4
AV-data2vec	1759h	30h	103M	CE	37.8	3.7	3.3
<i>Self-supervised (Large Models)</i>							
AV-HuBERT (Shi et al., 2022a)	433h	30h	325M	CE	44.8	4.5	4.2 ²
AV-data2vec	433h	30h	325M	CE	40.5	3.7	3.4
AV-HuBERT (Shi et al., 2022a;b)	1759h	30h	325M	CE	32.5	2.9	3.3
RAVen (Haliassos et al., 2022)	1759h	30h	671M	CTC+CE	33.1	2.6	-
VATLM (Zhu et al., 2022)	1759h ¹	30h	325M	CE	31.6	-	2.7
AV-data2vec	1759h	30h	325M	CE	30.8	2.7	2.7

¹ VATLM uses additional 3846h audio, 452h audio-text and 600M text data

² We reproduced AV-HuBERT and report our AVSR results.

data, larger models result in better performance. However, the benefits of increased model capacity and more pretraining data begin to diminish as can be seen in the results of the largest setting (Large model, 1759h pretraining data).

5.2. High-labeled Data Setup

Results of the high-labeled data setting (433h) are shown in Table. 2. AV-data2vec achieves state-of-the-art VSR/ASR/AVSR results except for the largest setting (Large model, 1759h pretraining data): u-HuBERT (Hsu & Shi, 2022) achieves the best VSR performance of 27.2, however, it uses an additional 452h of data for pretraining. VATLM (Zhu et al., 2022) and u-HuBERT achieve the best AVSR results, however, VATLM uses additional 3846h audio, 452h audio-text and 600M text data, which gives it an advantage. AV-HuBERT still delivers the best ASR performance of 1.3. However, the differences are tiny among all approaches, which we believe to be because of larger model capacity and more pretraining data.

5.3. Comparison to RAVen

Similar to AV-data2vec, RAVen (Haliassos et al., 2022) also uses contextualized and continuous targets, however, it differs from AV-data2vec in several important aspects. RAVen does not create joint modality embeddings and is not able to perform AVSR. Also, RAVen has different encoders for audio and video. For the Base model, each of the two encoders is half the size of AV-data2vec but collectively they have similar size. For the Large model, each RAVen encoder is the same size as AV-data2vec and thus the total size of RAVen in the Large size is about double of AV-data2vec. Next, the finetuning criterion for RAVen is joint CTC-Attention (Watanabe et al., 2017) while AV-data2vec

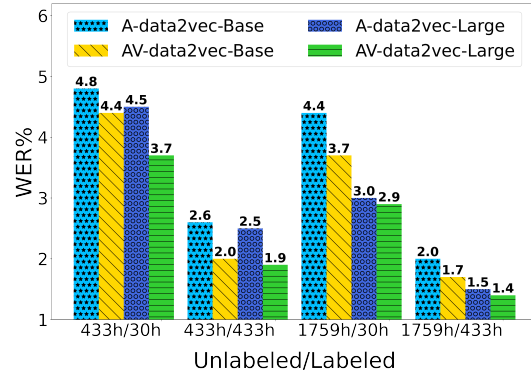


Figure 2. Audio-visual pretraining (AV-data2vec) performs better than audio-only training (A-data2vec) in almost all settings.

adopts a sequence to sequence architecture inline with AV-HuBERT (Shi et al., 2022a) and VATLM (Zhu et al., 2022). Finally, AV-data2vec empirically performs better as our results show.

5.4. Joint-modality vs. Audio-only Pretraining

Next, we compare joint audio-visual self-supervised learning to audio-only self-supervised learning. To do so, we pretrain an audio-only version of our model (A-data2vec), by simply removing visual features before they are fed to the transformer encoder; we do not use modality dropout. We train A-data2vec for 600K updates for all settings and adopt the same finetuning/decoding configurations as AV-data2vec. The results (Figure 2) show that joint audio-visual pretraining outperforms audio-only pretraining in almost all settings. In the largest high-resource setting (Large, 1759h unlabeled data, 433h labeled data), performance saturates

Table 2. High-labeled Data Results. We pretrain Base/Large models with 433h/1759h of unlabeled data and finetune on 433h of labeled data. Results of supervised/semi-supervised work are also included. AV-data2vec achieves state-of-the-art results under most settings.

Methods	Unlabeled AV data	Labeled Data	Backbone	Encoder Size	Criterion	VSR	ASR	AVSR
<i>Supervised</i>								
Afouras et al. (2018a)	-	1519h	Transformer	-	CE	58.9	8.3	-
Xu et al. (2020)	-	590h	RNN	-	CE	57.8	7.2	-
Shillingford et al. (2018)	-	3886h	RNN	-	CTC	55.1	-	-
Ma et al. (2022)	-	813h	Conformer	-	CTC+CE	34.7	-	-
Makino et al. (2019)	-	31000	RNN	-	Transducer	33.6	4.8	4.5
Prajwal et al. (2022)	-	2676h	Transformer	-	CE	30.7	-	-
Serdyuk et al. (2021)	-	90000h	Transformer	-	Transducer	25.9	-	2.3
Serdyuk et al. (2022)	-	90000h	Conformer	-	Transducer	17.0	-	1.6
<i>Semi-Supervised</i>								
Afouras et al. (2020)	344h	433h	Jasper(CNN)	-	CTC+CE	59.8	-	-
Ma et al. (2022)	641h	818h	Conformer	-	CTC+CE	31.5	-	-
<i>Self-supervised (Base Models)</i>								
AV-HuBERT (Shi et al., 2022a)	433h	433h	Transformer	103M	CE	44.0	3.0	2.8 ²
RAven (Haliassos et al., 2022)	433h	433h	Transformer	97M	CTC+CE	39.1	2.2	-
AV-data2vec	433h	433h	Transformer	103M	CE	39.0	2.0	1.8
AV-HuBERT (Shi et al., 2022a)	1759h	433h	Transformer	103M	CE	34.8	2.0	1.8 ³
RAven (Haliassos et al., 2022)	1759h	433h	Transformer	97M	CTC+CE	33.1	1.9	-
VATLM (Zhu et al., 2022)	1759h ¹	433h	Transformer	103M	CE	34.2	-	1.7
AV-data2vec	1759h	433h	Transformer	103M	CE	32.9	1.7	1.4
<i>Self-supervised (Large Models)</i>								
AV-HuBERT (Shi et al., 2022a)	433h	433h	Transformer	325M	CE	41.6	2.7	2.5 ²
AV-data2vec	433h	433h	Transformer	325M	CE	37.4	1.9	1.7
AV-HuBERT (Shi et al., 2022a;b)	1759h	433h	Transformer	325M	CE	28.6	1.3	1.4
RAven (Haliassos et al., 2022)	1759h	433h	Transformer	671M	CTC+CE	28.2	1.4	-
VATLM (Zhu et al., 2022)	1759h ¹	433h	Transformer	325M	CE	28.4	-	1.2
u-HuBERT (Hsu & Shi, 2022)	1759h ¹	433h	Transformer	325M	CE	27.2	1.4	1.2
AV-data2vec	1759h	433h	Transformer	325M	CE	28.5	1.4	1.3

¹ VATLM uses additional 3846h audio, 452h audio-text and 600M text data, and u-HuBERT uses additional 452h audio data.

² We reproduced AV-HuBERT to report corresponding AVSR results.

and the difference to audio-only pretraining is very small.

5.5. Ablations

Next, we ablate some of our hyper-parameter choices including how many blocks to average for the target representations, settings for the modality scheduler, EMA scheduler as well as batch size and learning rate. For faster experimentation, we adopt a Base model, pretrain on 433h of unlabeled data for 600k updates with the learning rate of 5e-4 and batch size of 640s.

5.5.1. TOP-K TARGET AVERAGING

We first measure the impact of creating contextualized target representations based on multiple blocks ranging from the top block to the 12 blocks. For this experiment, we fix $p_{AV} = 0.5$, $p_A = p_V = 0.25$ for the student encoder which is the default schedule of Shi et al. (2022a); we set $p_A = 1$, $p_{AV} = p_V = 0$ for the teacher encoder as video contains more ambiguous information as targets, as mentioned in Haliassos et al. (2022). For EMA, we set $\tau^s = 0.999$, $\tau^e = 0.99999$ and $\tau_{anneal} = 100k$. Fig.3 shows that averaging more blocks improves performance,

inline with prior experiments for ASR, image recognition and natural language understanding (Baevski et al., 2022b). We therefore generally use $K = 12$ for Base models and $K = 24$ for Large models.

5.5.2. MODALITY SCHEDULER

Next, we explore the modality dropout scheduler starting with the teacher encoder. To do so, we still fix $p_{AV} = 0.5$, $p_A = p_V = 0.25$ for the student encoder and vary the scheduler for teacher encoder only. For simplicity, we keep the teacher modality dropout values constant over pretraining and experiment with different values subject to the constraint $p_{AV} + p_A + p_V = 1$. We use the same EMA configuration as Sec. 5.5.1.

Table.3 shows that using only audio inputs for the teacher model gives the best performance for all tasks (VSR, ASR, AVSR). We also find that introducing video data into target representations always tends to harm the performance. We speculate that visual targets introduce some ambiguity which harms training. Based on this, we use audio-only inputs for the teacher model for all other experiments.

Next, we vary the hyper-parameters for the student modal-

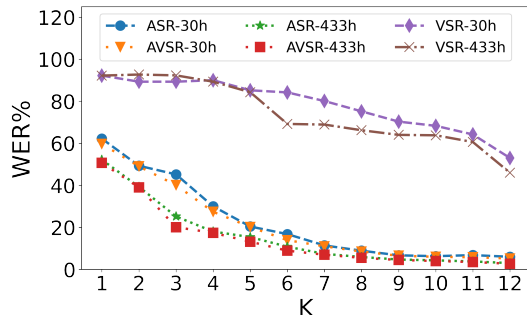


Figure 3. Effect of averaging K blocks to create contextualized target representations. More blocks improve performance because targets become richer due to including both high-level and low-level features. Results are based on a Base model pretrained on 433h of unlabeled data and finetuned on 30h of labeled data.

ity scheduler. Table.4, the best results are achieved in the case where more probability is given for audio-video in the beginning and more probability is given for video-only in the end. The annealing steps is 150k. We detail the student modality scheduler in Appendix. A.1.

5.5.3. EMA SCHEDULER

We also investigate the effect of the EMA parameters (τ^s , τ^e , τ_{anneal}). We only vary τ_e and τ_{anneal} while fixing the other configurations same as the best setting in Sec. 5.5.2. Results in Table. 5 show that the best configuration is $\tau^s = 0.999$, $\tau^e = 0.99999$, $\tau_{anneal} = 100k$ and best results are 51.1 for VSR, 5.2 for ASR and 5.0 for AVSR.

Teacher modality scheduler			30h Labeled Data		
p_{AV}	p_V	p_A	VSR	ASR	AVSR
0	0	1	53.2	6.2	6.0
0	1	0	83.2	40.2	40.0
1	0	0	74.8	24.4	22.7
0.5	0	0.5	59.0	8.5	8.2
0	0.5	0.5	63.2	9.2	8.7
0.25	0.25	0.5	61.6	8.8	8.4

Table 3. Effect of modality dropout schedules for the teacher model: audio-only targets achieve the best results. p_{AV} , p_V and p_A are constant. .

Student modality scheduler			30h Labeled Data		
p_{AV}	p_V	p_A	VSR	ASR	AVSR
0.5→0.5	0.25→0.25	0.25→0.25	53.2	6.2	6.0
0→0	1→1	0→0	64.3	36.1	34.8
1→1	0→0	0→0	66.8	12.2	10.3
0→0	0→0	1→1	95.7	5.2	10.3
1→0.25	0→0.75	0→0	52.4	5.5	5.3
0.25→1	0.75→0	0→0	57.6	5.5	5.2
0.5→0.5	0→0.25	0.5→0.25	54.5	6.8	6.6
1→0.25	0→0.5625	0→0.1875	57.1	6.0	5.5

Table 4. Effect of modality dropout schedules for the student model. p_{AV} is linearly annealed for 150k. p_V and p_A are quadratically annealed for 150k. However, most of p_V and p_A are actually still linearly annealed in our examples as shown in Appendix. A.1.

EMA Scheduler			30h Labeled Data		
τ_s	τ_e	τ_{anneal}	VSR	ASR	AVSR
0.999	0.99999	100k	51.1	5.2	5.0
0.999	0.99999	200k	53.7	5.7	5.5
0.999	0.99995	100k	53.5	6.2	5.9
0.999	0.99995	200k	54.0	6.9	6.3
0.999	1	100k	67.8	13.4	10.7
0.999	1	200k	70.6	18.0	8.4

Table 5. Effect of EMA Scheduler.

5.5.4. ABLATIONS FOR SCALING

For Large models and the largest unlabeled data setting (1759h), we investigate the effect of batch size and learning rates. Table.6 shows the performance of a few settings we explored: For 433h pretraining with Base model settings, increasing the batch size leads to plateauing performance. However, when the amount of pretraining data is increased to 1759h, larger batch size still leads to better performance for all tasks.

For the Large model with 433h of unlabeled data, we found that smaller learning rates ($<5e-4$) improve performance; we find that $2e-4$ gives the best performance. When increasing the amount of pretraining data to 1759h, the largest batch size we considered (2560s) with learning rate $2e-4$ performs very well.

unlabeled	Configuration			30h Labeled Data			433h Labeled Data		
	bsz	lr	model	VSR	ASR	AVSR	VSR	ASR	AVSR
433h	640s	5e-4	BASE	48.7	4.9	4.7	40.6	2.2	2.0
433h	1280s	5e-4	BASE	45.2	4.4	4.2	39.0	2.0	1.8
433h	2560s	5e-4	BASE	45.3	4.5	4.3	39.1	2.0	1.8
1759h	640s	5e-4	BASE	52.2	4.9	4.6	39.6	3.2	3.0
1759h	1280s	5e-4	BASE	44.2	4.2	4.0	35.0	2.8	2.6
1759h	2560s	5e-4	BASE	37.8	3.7	3.3	32.9	1.7	1.4
433h	1280s	5e-4	BASE	45.5	4.3	4.1	40.2	2.2	2.0
433h	1280s	3e-4	LARGE	43.7	4.0	3.8	39.8	2.0	1.9
433h	1280s	2e-4	LARGE	40.5	3.7	3.4	37.4	1.9	1.7
433h	1280s	1e-4	LARGE	41.2	3.9	3.8	38.8	2.3	2.1
1759h	2560s	2e-4	LARGE	30.8	2.7	2.7	28.5	1.4	1.3

Table 6. Ablation of batch size and learning rates for Base and Large models. bsz denotes batch size. Large models benefit more from smaller learning rates and larger amounts of unlabeled data benefits more from larger batch size.

6. Conclusion and Future work

We proposed AV-data2vec, a self-supervised framework to jointly learn audio-visual speech representations based on contextualized targets. AV-data2vec adopts a shared modality-agnostic transformer encoder which takes as input both audio and video data, both of which are fused early on, similar to the human speech perception system. AV-data2vec unifies ASR, VSR and AVSR within a single framework and achieves state-of-the-art performance under most settings. Future work includes data-efficient and model-efficient training, considering both natural sound as well as instructional audio as well as more general tasks such as image recognition and sound classification.

7. Acknowledgement

We thank Bernie Huang for fruitful discussions around transformer block normalization schemes. The purpose of this project is foremost to further the state of the art in audio-visual representation learning research.

References

- Afouras, T., Chung, J. S., Senior, A., Vinyals, O., and Zisserman, A. Deep audio-visual speech recognition. *IEEE transactions on pattern analysis and machine intelligence*, 2018a.
- Afouras, T., Chung, J. S., and Zisserman, A. Lrs3-ted: a large-scale dataset for visual speech recognition. *arXiv preprint arXiv:1809.00496*, 2018b.
- Afouras, T., Chung, J. S., and Zisserman, A. Asr is all you need: Cross-modal distillation for lip reading. In *ICASSP 2020-2020 IEEE International Conference on Acoustics, Speech and Signal Processing (ICASSP)*, pp. 2143–2147. IEEE, 2020.
- Akbari, H., Yuan, L., Qian, R., Chuang, W.-H., Chang, S.-F., Cui, Y., and Gong, B. Vatt: Transformers for multimodal self-supervised learning from raw video, audio and text. *Advances in Neural Information Processing Systems*, 34: 24206–24221, 2021.
- Alayrac, J.-B., Donahue, J., Luc, P., Miech, A., Barr, I., Hasson, Y., Lenc, K., Mensch, A., Millican, K., Reynolds, M., et al. Flamingo: a visual language model for few-shot learning. *arXiv preprint arXiv:2204.14198*, 2022.
- Ao, J., Wang, R., Zhou, L., Liu, S., Ren, S., Wu, Y., Ko, T., Li, Q., Zhang, Y., Wei, Z., et al. Specht5: Unified-modal encoder-decoder pre-training for spoken language processing. *arXiv preprint arXiv:2110.07205*, 2021.
- Baevski, A., Auli, M., and Mohamed, A. Effectiveness of self-supervised pre-training for speech recognition. *arXiv preprint arXiv:1911.03912*, 2019a.
- Baevski, A., Schneider, S., and Auli, M. vq-wav2vec: Self-supervised learning of discrete speech representations. *arXiv preprint arXiv:1910.05453*, 2019b.
- Baevski, A., Zhou, Y., Mohamed, A., and Auli, M. wav2vec 2.0: A framework for self-supervised learning of speech representations. *Advances in Neural Information Processing Systems*, 33:12449–12460, 2020.
- Baevski, A., Babu, A., Hsu, W.-N., and Auli, M. Efficient self-supervised learning with contextualized target representations for vision, speech and language. *arXiv preprint arXiv:2212.07525*, 2022a.
- Baevski, A., Hsu, W.-N., Xu, Q., Babu, A., Gu, J., and Auli, M. Data2vec: A general framework for self-supervised learning in speech, vision and language. *arXiv preprint arXiv:2202.03555*, 2022b.
- Bahdanau, D., Chorowski, J., Serdyuk, D., Brakel, P., and Bengio, Y. End-to-end attention-based large vocabulary speech recognition. In *2016 IEEE international conference on acoustics, speech and signal processing (ICASSP)*, pp. 4945–4949. IEEE, 2016.
- Bapna, A., Chung, Y.-a., Wu, N., Gulati, A., Jia, Y., Clark, J. H., Johnson, M., Riesa, J., Conneau, A., and Zhang, Y. Slam: A unified encoder for speech and language modeling via speech-text joint pre-training. *arXiv preprint arXiv:2110.10329*, 2021.
- Bernstein, L. E. and Liebenthal, E. Neural pathways for visual speech perception. *Frontiers in neuroscience*, 8: 386, 2014.
- Calvert, G., Bullmore, E., Brammer, M., Campbell, R., Iversen, S., Woodruff, P., McGuire, P., Williams, S., and David, A. Silent lipreading activates the auditory cortex. *Science*, 276:593–596, 1997.
- Caron, M., Touvron, H., Misra, I., Jégou, H., Mairal, J., Bojanowski, P., and Joulin, A. Emerging properties in self-supervised vision transformers. In *Proceedings of the IEEE/CVF International Conference on Computer Vision*, pp. 9650–9660, 2021.
- Chan, D. M., Ghosh, S., Chakrabarty, D., and Hoffmeister, B. Multi-modal pre-training for automated speech recognition. In *ICASSP 2022-2022 IEEE International Conference on Acoustics, Speech and Signal Processing (ICASSP)*, pp. 246–250. IEEE, 2022.
- Chen, S., Wang, C., Chen, Z., Wu, Y., Liu, S., Chen, Z., Li, J., Kanda, N., Yoshioka, T., Xiao, X., Wu, J., Zhou, L., Ren, S., Qian, Y., Qian, Y., Wu, J., Zeng, M., Yu, X., and Wei, F. Wavlm: Large-scale self-supervised pre-training for full stack speech processing. *IEEE Journal of Selected Topics in Signal Processing*, 16(6):1505–1518, 2022a.
- Chen, Z., Zhang, Y., Rosenberg, A., Ramabhadran, B., Moreno, P., Bapna, A., and Zen, H. Maestro: Matched speech text representations through modality matching. *arXiv preprint arXiv:2204.03409*, 2022b.
- Chung, J. S., Nagrani, A., and Zisserman, A. Voxceleb2: Deep speaker recognition. *arXiv preprint arXiv:1806.05622*, 2018.
- Chung, Y.-A. and Glass, J. Generative pre-training for speech with autoregressive predictive coding. In *ICASSP 2020-2020 IEEE International Conference on Acoustics, Speech and Signal Processing (ICASSP)*, pp. 3497–3501. IEEE, 2020.

- Chung, Y.-A., Tang, H., and Glass, J. Vector-quantized autoregressive predictive coding. *arXiv preprint arXiv:2005.08392*, 2020.
- Devlin, J., Chang, M.-W., Lee, K., and Toutanova, K. Bert: Pre-training of deep bidirectional transformers for language understanding. *arXiv preprint arXiv:1810.04805*, 2018.
- Diehl, R. L., Lotto, A. J., Holt, L. L., et al. Speech perception. *Annual review of psychology*, 55(1):149–179, 2004.
- Dou, Z.-Y., Xu, Y., Gan, Z., Wang, J., Wang, S., Wang, L., Zhu, C., Zhang, P., Yuan, L., Peng, N., et al. An empirical study of training end-to-end vision-and-language transformers. In *Proceedings of the IEEE/CVF Conference on Computer Vision and Pattern Recognition*, pp. 18166–18176, 2022.
- Fang, H., Xiong, P., Xu, L., and Chen, Y. Clip2video: Mastering video-text retrieval via image clip. *arXiv preprint arXiv:2106.11097*, 2021.
- Fowler, C. A. and Dekle, D. J. Listening with eye and hand: cross-modal contributions to speech perception. *Journal of experimental psychology: Human perception and performance*, 17(3):816, 1991.
- Green, K. The use of auditory and visual information during phonetic processing: implications for theories of speech perception. campbell r, dodd b, burnham d, editors. hearing by eye ii: advances in the psychology of speechreading and auditory–visual speech, 1998.
- Grill, J.-B., Strub, F., Alché, F., Tallec, C., Richemond, P., Buchatskaya, E., Doersch, C., Avila Pires, B., Guo, Z., Gheshlaghi Azar, M., et al. Bootstrap your own latent-a new approach to self-supervised learning. *Advances in neural information processing systems*, 33:21271–21284, 2020.
- Gulati, A., Qin, J., Chiu, C.-C., Parmar, N., Zhang, Y., Yu, J., Han, W., Wang, S., Zhang, Z., Wu, Y., et al. Conformer: Convolution-augmented transformer for speech recognition. *arXiv preprint arXiv:2005.08100*, 2020.
- Haliassos, A., Ma, P., Mira, R., Petridis, S., and Pantic, M. Jointly learning visual and auditory speech representations from raw data. *arXiv preprint arXiv:2212.06246*, 2022.
- He, K., Zhang, X., Ren, S., and Sun, J. Delving deep into rectifiers: Surpassing human-level performance on imagenet classification. In *Proceedings of the IEEE international conference on computer vision*, pp. 1026–1034, 2015.
- He, K., Zhang, X., Ren, S., and Sun, J. Deep residual learning for image recognition. In *Proceedings of the IEEE conference on computer vision and pattern recognition*, pp. 770–778, 2016.
- Hockett, C. F. and Hockett, C. D. The origin of speech. *Scientific American*, 203(3):88–97, 1960.
- Hsu, W.-N. and Shi, B. u-hubert: Unified mixed-modal speech pretraining and zero-shot transfer to unlabeled modality. In *Advances in Neural Information Processing Systems*, 2022.
- Hsu, W.-N., Bolte, B., Tsai, Y.-H. H., Lakhotia, K., Salakhutdinov, R., and Mohamed, A. Hubert: Self-supervised speech representation learning by masked prediction of hidden units. *IEEE/ACM Transactions on Audio, Speech, and Language Processing*, 29:3451–3460, 2021.
- Ioffe, S. and Szegedy, C. Batch normalization: Accelerating deep network training by reducing internal covariate shift. In *International conference on machine learning*, pp. 448–456. PMLR, 2015.
- King, D. E. Dlib-ml: A machine learning toolkit. *The Journal of Machine Learning Research*, 10:1755–1758, 2009.
- Kudo, T. Subword regularization: Improving neural network translation models with multiple subword candidates. *arXiv preprint arXiv:1804.10959*, 2018.
- Li, L. H., Yatskar, M., Yin, D., Hsieh, C.-J., and Chang, K.-W. Visualbert: A simple and performant baseline for vision and language. *arXiv preprint arXiv:1908.03557*, 2019.
- Li, Y., Fan, H., Hu, R., Feichtenhofer, C., and He, K. Scaling language-image pre-training via masking. *arXiv preprint arXiv:2212.00794*, 2022.
- Ling, S., Liu, Y., Salazar, J., and Kirchhoff, K. Deep contextualized acoustic representations for semi-supervised speech recognition. In *ICASSP 2020-2020 IEEE International Conference on Acoustics, Speech and Signal Processing (ICASSP)*, pp. 6429–6433. IEEE, 2020.
- Liu, A. H., Chung, Y.-A., and Glass, J. Non-autoregressive predictive coding for learning speech representations from local dependencies. *arXiv preprint arXiv:2011.00406*, 2020.
- Luo, H., Ji, L., Shi, B., Huang, H., Duan, N., Li, T., Li, J., Bharti, T., and Zhou, M. Univl: A unified video and language pre-training model for multimodal understanding and generation. *arXiv preprint arXiv:2002.06353*, 2020.

- Luo, H., Ji, L., Zhong, M., Chen, Y., Lei, W., Duan, N., and Li, T. Clip4clip: An empirical study of clip for end to end video clip retrieval. *arXiv preprint arXiv:2104.08860*, 2021.
- Ma, P., Petridis, S., and Pantic, M. Visual speech recognition for multiple languages in the wild. *arXiv preprint arXiv:2202.13084*, 2022.
- Makino, T., Liao, H., Assael, Y., Shillingford, B., Garcia, B., Braga, O., and Siohan, O. Recurrent neural network transducer for audio-visual speech recognition. In *2019 IEEE automatic speech recognition and understanding workshop (ASRU)*, pp. 905–912. IEEE, 2019.
- McGurk, H. and MacDonald, J. Hearing lips and seeing voices. *Nature*, 264(5588):746–748, 1976.
- Musacchia, G., Sams, M., Nicol, T., and Kraus, N. Seeing speech affects acoustic information processing in the human brainstem. *Experimental Brain Research*, 168(1): 1–10, 2006.
- Oord, A. v. d., Li, Y., and Vinyals, O. Representation learning with contrastive predictive coding. *arXiv preprint arXiv:1807.03748*, 2018.
- Ott, M., Edunov, S., Baevski, A., Fan, A., Gross, S., Ng, N., Grangier, D., and Auli, M. fairseq: A fast, extensible toolkit for sequence modeling. *arXiv preprint arXiv:1904.01038*, 2019.
- Petridis, S., Stafylakis, T., Ma, P., Tzimiropoulos, G., and Pantic, M. Audio-visual speech recognition with a hybrid ctc/attention architecture. In *2018 IEEE Spoken Language Technology Workshop (SLT)*, pp. 513–520. IEEE, 2018.
- Prajwal, K., Afouras, T., and Zisserman, A. Sub-word level lip reading with visual attention. In *Proceedings of the IEEE/CVF Conference on Computer Vision and Pattern Recognition*, pp. 5162–5172, 2022.
- Radford, A., Kim, J. W., Hallacy, C., Ramesh, A., Goh, G., Agarwal, S., Sastry, G., Askell, A., Mishkin, P., Clark, J., et al. Learning transferable visual models from natural language supervision. In *International Conference on Machine Learning*, pp. 8748–8763. PMLR, 2021.
- Radford, A., Kim, J. W., Xu, T., Brockman, G., McLeavey, C., and Sutskever, I. Robust speech recognition via large-scale weak supervision. *arXiv preprint arXiv:2212.04356*, 2022.
- Schneider, S., Baevski, A., Collobert, R., and Auli, M. wav2vec: Unsupervised pre-training for speech recognition. *arXiv preprint arXiv:1904.05862*, 2019.
- Seddik, A. F., El Adawy, M., and Ismail, A. A robust speech disorders correction system for arabic language using visual speech recognition. *Biomed Res*, 24:2, 2013.
- Serdyuk, D., Braga, O., and Siohan, O. Transformer-based video front-ends for audio-visual speech recognition. *arXiv preprint arXiv:2201.10439*, 2022.
- Serdyuk, D. D., Siohan, O., and Braga, O. d. P. F. Audio-visual speech recognition is worth 32x32x8 voxels. *arXiv preprint arXiv:2109.09536*, 2021.
- Shi, B., Hsu, W.-N., Lakhota, K., and Mohamed, A. Learning audio-visual speech representation by masked multimodal cluster prediction. *arXiv preprint arXiv:2201.02184*, 2022a.
- Shi, B., Hsu, W.-N., and Mohamed, A. Robust self-supervised audio-visual speech recognition. *arXiv preprint arXiv:2201.01763*, 2022b.
- Shillingford, B., Assael, Y., Hoffman, M. W., Paine, T., Hughes, C., Prabhu, U., Liao, H., Sak, H., Rao, K., Bennett, L., et al. Large-scale visual speech recognition. *arXiv preprint arXiv:1807.05162*, 2018.
- Summerfield, Q. Lipreading and audio-visual speech perception. *Philosophical Transactions of the Royal Society of London. Series B: Biological Sciences*, 335(1273):71–78, 1992.
- Sun, C., Myers, A., Vondrick, C., Murphy, K., and Schmid, C. Videobert: A joint model for video and language representation learning. In *Proceedings of the IEEE/CVF International Conference on Computer Vision*, pp. 7464–7473, 2019.
- Van Den Oord, A., Vinyals, O., et al. Neural discrete representation learning. *Advances in neural information processing systems*, 30, 2017.
- Wang, Z., Yu, J., Yu, A. W., Dai, Z., Tsvetkov, Y., and Cao, Y. Simvlm: Simple visual language model pretraining with weak supervision. *arXiv preprint arXiv:2108.10904*, 2021.
- Watanabe, S., Hori, T., Kim, S., Hershey, J. R., and Hayashi, T. Hybrid ctc/attention architecture for end-to-end speech recognition. *IEEE Journal of Selected Topics in Signal Processing*, 11(8):1240–1253, 2017.
- Xu, B., Lu, C., Guo, Y., and Wang, J. Discriminative multi-modality speech recognition. In *Proceedings of the IEEE/CVF Conference on Computer Vision and Pattern Recognition*, pp. 14433–14442, 2020.
- Xu, H., Ghosh, G., Huang, P.-Y., Okhonko, D., Aghajanyan, A., Metze, F., Zettlemoyer, L., and Feichtenhofer, C.

Videoclip: Contrastive pre-training for zero-shot video-text understanding. *arXiv preprint arXiv:2109.14084*, 2021.

Yang, J., Duan, J., Tran, S., Xu, Y., Chanda, S., Chen, L., Zeng, B., Chilimbi, T., and Huang, J. Vision-language pre-training with triple contrastive learning. In *Proceedings of the IEEE/CVF Conference on Computer Vision and Pattern Recognition*, pp. 15671–15680, 2022.

Yue, X. and Li, H. Phonetically motivated self-supervised speech representation learning. In *Interspeech*, pp. 746–750, 2021.

Zellers, R., Lu, J., Lu, X., Yu, Y., Zhao, Y., Salehi, M., Kusupati, A., Hessel, J., Farhadi, A., and Choi, Y. Merlot reserve: Neural script knowledge through vision and language and sound. In *Proceedings of the IEEE/CVF Conference on Computer Vision and Pattern Recognition*, pp. 16375–16387, 2022.

Zeng, Y., Zhang, X., and Li, H. Multi-grained vision language pre-training: Aligning texts with visual concepts. *arXiv preprint arXiv:2111.08276*, 2021.

Zhang, Z., Zhou, L., Ao, J., Liu, S., Dai, L., Li, J., and Wei, F. Speechut: Bridging speech and text with hidden-unit for encoder-decoder based speech-text pre-training. *arXiv preprint arXiv:2210.03730*, 2022.

Zhu, Q., Zhou, L., Zhang, Z., Liu, S., Jiao, B., Zhang, J., Dai, L., Jiang, D., Li, J., and Wei, F. Vatlm: Visual-audio-text pre-training with unified masked prediction for speech representation learning. *arXiv preprint arXiv:2211.11275*, 2022.

A. Appendix

A.1. Modality Dropout Scheduler

Since the teacher modality scheduler is fixed to be audio-only, we primarily discuss the student modality dropout. As mentioned in Section 3.2, p_{AV} , $p_{V|\bar{A}V}$ and $p_{A|\bar{A}V}$ are linearly annealed while p_V and p_A are quadratically annealed, subject to $p_{AV} + p_V + p_A = 1$. However, most of p_V and p_A are actually still linearly annealed in our examples. In the following, we visualize the student schedulers for both p_{AV}, p_A, p_V and $p_{AV}, p_{V|\bar{A}V}, p_{A|\bar{A}V}$. The first one is the actual scheduler and the second one the implemented scheduler in the algorithm. We list the schedulers for all results shown in Table 4.

A.1.1. $p_{AV} : 0.5 \rightarrow 0.5, p_V : 0.25 \rightarrow 0.25, p_A : 0.25 \rightarrow 0.25$ OVER 150K

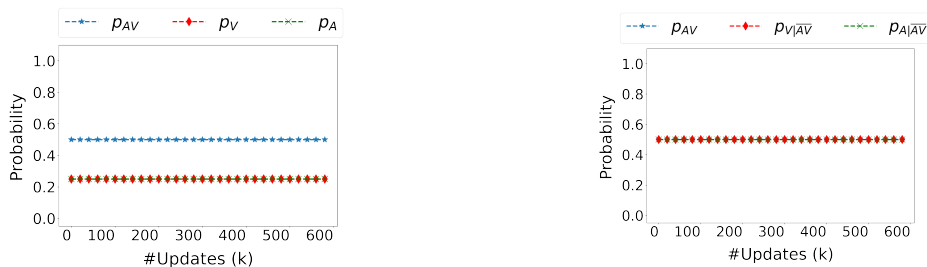


Figure 4. VSR=53.2, ASR=6.2, AVSR=6.0

A.1.2. $p_{AV} : 0 \rightarrow 0, p_V : 1 \rightarrow 1, p_A : 0 \rightarrow 0$ OVER 150K



Figure 5. VSR=64.3, ASR=36.1, AVSR=34.8

A.1.3. $p_{AV} : 1 \rightarrow 1, p_V : 0 \rightarrow 0, p_A : 0 \rightarrow 0$ OVER 150K



Figure 6. VSR=66.8, ASR=12.2, AVSR=10.3

A.1.4. $p_{AV} : 0 \rightarrow 0, p_V : 0 \rightarrow 0, p_A : 1 \rightarrow 1$ OVER 150K



Figure 7. VSR=95.7, ASR=5.2, AVSR=10.3

A.1.5. $p_{AV} : 1 \rightarrow 0.25$, $p_V : 0 \rightarrow 0.75$, $p_A : 0 \rightarrow 0$ OVER 150K

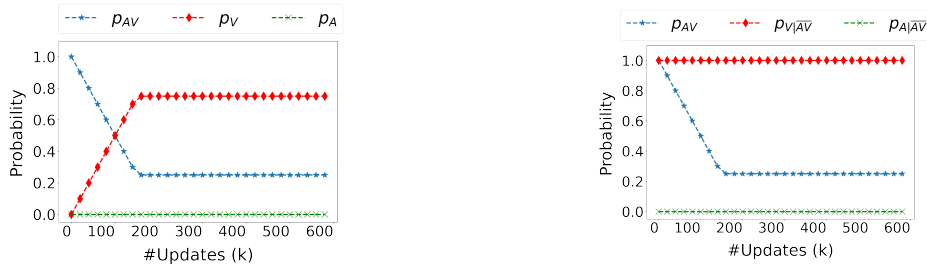


Figure 8. VSR=52.4, ASR=5.5, AVSR=5.3

A.1.6. $p_{AV} : 0.25 \rightarrow 1$, $p_V : 0.75 \rightarrow 0$, $p_A : 0 \rightarrow 0$ OVER 150K

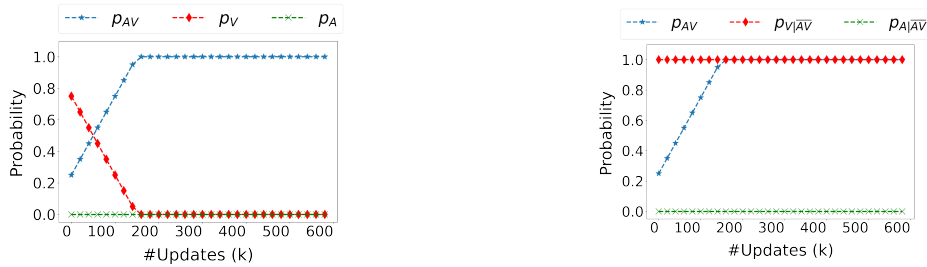


Figure 9. VSR=57.6, ASR=5.5, AVSR=5.2

A.1.7. $p_{AV} : 0.5 \rightarrow 0.5$, $p_V : 0 \rightarrow 0.25$, $p_A : 0.5 \rightarrow 0.25$ OVER 150K



Figure 10. VSR=54.5, ASR=6.8, AVSR=6.6

A.1.8. $p_{AV} : 1 \rightarrow 0.25$, $p_V : 0 \rightarrow 0.5625$, $p_A : 0 \rightarrow 0.1875$ OVER 150K

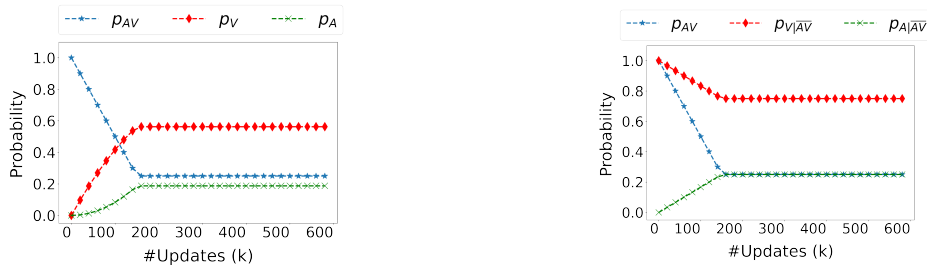


Figure 11. VSR=57.1, ASR=6.0, AVSR=5.5

The scheduler 8 is finally used for all settings (Large/Base, 1759h/433h unlabeled), with the exception that that actual total number of updates is 1000k for Base Model/433h and 2000k for the others.